Available online at www.sciencedirect.com
ScienceDirect
Biomaterials 28 (2007) 2368–2377
Biomaterials
www.elsevier.com/locate/biomaterials

Protein mapping of calcium carbonate biominerals by immunogold

Frédéric Marin[a,*], Boaz Pokroy[b], Gilles Luquet[a], Pierre Layrolle[c], Klaas De Groot[d]

[a]*UMR CNRS 5561 "Biogéosciences", Université de Bourgogne, 6 Boulevard Gabriel 21000 DIJON, France*
[b]*Department of Materials Engineering, Technion-Israël Institute of Technology, Haifa 32000, Israël*
[c]*INSERM U791, Osteoarticular and Dental Tissue Engineering, Faculty of Dental Surgery, Place Alexis Ricordeau, 44042 Nantes, France*
[d]*University of Twente, Institute for Biomedical Technology, Professor Bronkhorstlaan 10D, 3723 MB Bilthoven, The Netherlands*

Received 13 November 2006; accepted 23 January 2007
Available online 2 February 2007

Abstract

The construction of metazoan calcium carbonate skeletons is finely regulated by a proteinaceous extracellular matrix, which remains embedded within the exoskeleton. In spite of numerous biochemical studies, the precise localization of skeletal proteins has remained for a long time as an elusive goal. In this paper, we describe a technique for visualizing shell matrix proteins on the surface of calcium carbonate crystals or within the biominerals. The technique is as follows: freshly broken pieces of biominerals or NaOCl then EDTA-etched polished surfaces are incubated with an antibody elicited against one matrix protein, then with a secondary gold-coupled antibody. After silver enhancement, the samples are subsequently observed with scanning electron microscopy by using back-scattered electron mode. In the present case, the technique is applied to a particular example, the calcitic prisms that compose the outer shell layer of the mediterranean fan mussel *Pinna nobilis*. One major soluble protein, caspartin, which was identified recently, was partly *de novo* sequenced after enzymatic digestions. A polyclonal antibody raised against caspartin was used for its localization within and on the prisms. The immunogold localization indicated that caspartin surrounds the calcitic prisms, but is also dispersed within the biominerals. This example illustrates the deep impact of the technique on the definition of intracrystalline versus intercrystalline matrix proteins. Furthermore, it is an important tool for assigning a putative function to a matrix protein of interest.

Keywords: Calcium carbonate; Immunogold; SEM; Caspartin; Back-scattered electrons; Surface treatment

1. Introduction

In the metazoan world, calcium carbonate skeletons are the most commonly encountered biomineralizations, from the most "simple" diploblastic animals, sponges and corals, to deuterostomes, echinoderms and vertebrates. Their study offers promising perspectives in biotechnology: the synthesis at room temperature of materials that mimic the molluscan nacre, both in its structure and in its superior mechanical properties [1,2]; the use of bioactive coral or mollusk implants in bone substitution medicine [3,4].

All metazoan calcium carbonate biomineralizations share a remarkable property. They are organo-mineral assemblages, where the dominant mineral—calcite, aragonite, or less frequently, other polymorphs of $CaCO_3$—is closely associated with a minor organic matrix [5]. This latter (0.1–5 wt% of the skeleton) represents a mixture of proteins, glycoproteins and polysaccharides, which are secreted by the calcifying tissues during skeletogenesis, and sealed within the skeleton during its growth. The matrix displays essential functions in biomineralization: beside physico-chemical interactions, i.e., nucleation, polymorph selection, crystal growth and inhibition [6] the organic matrix is suspected to display enzymatic functions [7] and to be involved in cell signaling [8].

One fundamental aspect in biomineralization research is the comprehension of the topographic relations between the organic and the mineral phases [6]. Localizing the matrix components around and within biominerals helps to understand how they interact together, giving thus information on putative functions of matrix components during crystal synthesis. The precise localization of matrix components is critical, since it is usually the basis from

*Corresponding author. Tel.: +33 3 80 39 63 72; fax: +33 3 80 39 63 87.
E-mail address: frederic.marin@u-bourgogne.fr (F. Marin).

0142-9612/$ - see front matter © 2007 Elsevier Ltd. All rights reserved.
doi:10.1016/j.biomaterials.2007.01.029

which new models of biomineralization are proposed. The best example is that of molluscan nacre, for which the "classical" model published in the early 1980s [9] evolved drastically until recently [10–13].

For localizing the organic matrix in calcium carbonate biominerals, several techniques are available from the most easy-to-handle to the most sophisticated ones: at low magnification, the distribution of organic matrix within biominerals can be visualized by coupling light microscopy with cathodoluminescence [14], with epifluorescence or by using different fluorochrome staining [15]. In the magnification range [1000–50,000], scanning electron microscopy (SEM) gives interesting results when samples surfaces are pre-treated for deciphering the fine topography of mineral-matrix assemblages [16]. At higher magnification, transmission electron microscopy (TEM) and cryo-TEM reveal nanostructural details [11,17], but their implementation requires a special expertize and skill. Finally, at the molecular scale, atomic force microscopy gives spectacular results, which however, may be difficult to interpret [18]. Other physical techniques, like high-resolution energy/wavelength dispersive X-ray analysis (EDX/WDX), Raman microspectroscopy, X-ray diffraction, X-ray absorption near edge structure spectroscopy (XANES), nanoscale secondary-ion mass spectrometry (NanoSIMS) may be useful. However, most of them do not localize a particular matrix component. At the best, XANES [19] and NanoSIMS [20] can only localize some chemical groups.

To localize a single component within a calcified skeleton, immunological techniques represent a valuable approach. The basic principle of these techniques is the use of antibody molecules, which specifically bind to their target antigens. The recognition domain of a given antibody is usually a short portion of the antigen, for polypeptides, 5–8 amino acids. The technique applied to skeletal matrices has not received a great deal of attention, in spite of having been successfully used with calcium carbonate biominerals: mollusc shells [21,22] and coral skeletons [23]. Two drawbacks of these earlier experiments were that, in two cases [21,23], the antibody preparations were made from crude mixtures of different matrix components and, if not, that these preparations were observed by optical microscopy, which implies a limited magnification [22].

In this paper, we describe an immunological staining, which overcomes these technical obstacles. The studied biominerals are the shell calcitic prisms of the pteriomorphid bivalve *Pinna nobilis*, from which caspartin, a shell soluble protein, was previously characterized [24]. In this paper, the characterization was pursued and caspartin was partly *de novo* sequenced after enzymatic digestions. Polyclonal antibodies were obtained against caspartin and used for immunogold localization with SEM, under back-scattered electron mode, after different surface treatments. We assess that this technique represents a substantial improvement for the localization of matrix components. Furthermore, it allows redefining the concepts of intracrystalline versus intercrystalline matrix.

2. Materials and methods

2.1. Materials

The shells of the bivalve *P. nobilis* were kindly provided by CERAM (Centre d'Etudes et de Recherches Animales Marines, Prof. Nardo Vicente). Like several Pteriomorphid bivalves, *P. nobilis* exhibits a nacro-prismatic shell microstructure. The surface of the shells was carefully cleaned by abrasion with a dental drill, and the two shell layers were separated mechanically. In this study, only the outer prismatic calcitic layer was used for subsequent observations. On the one hand, small shell fragments were used for immunogold assay. On the other hand, several fragments of the prismatic layer were treated for protein purification. In this second case, they were soaked in dilute sodium hypochlorite (0.2 wt% active chlorine), for 4 days, under constant stirring. This operation resulted in the isolation of the calcitic prismatic biocrystals by degrading their periprismatic organic sheath [24]. Prisms were collected on a membrane, extensively rinsed with Milli-Q water, dried and crushed under liquid nitrogen. The soluble matrix (intra-prismatic) was extracted from this powder preparation.

2.2. Shell protein purification and polyclonal antibodies

The intra-prismatic matrix was obtained by overnight dissolution of the prism powder (20 g) with cold dilute acetic acid (5% v/v, 4 °C). The clear solution (about 1 l) was centrifuged (4500 rpm, 10 min), ultra-filtered (10 kDa cut-off) and extensively dialyzed [24]. Caspartin, a 17 kDa-protein and one of the two main soluble macromolecules of the prisms, was obtained by a blind fractionation of the matrix on preparative gel electrophoresis, followed by a dot-blot detection as previously described [24]. The quality of the preparation was checked on mini denaturing electrophoresis gels (Bio Rad Protean III), which were subsequently stained with silver [24].

Sera containing polyclonal antibodies raised against caspartin were obtained from the purified caspartin, in a white rabbit, according to a standard protocol (Eurogentec, Seraing, Belgium). The immunization procedure was performed with injections at 0, 14, 28 and 56 days, and bleedings at 0, 38, 66 and 80 days. The sera (1st, 2nd and 3rd bleeding) were tested on ELISA for the determination of their respective titer. The specificity of each serum for caspartin was subsequently checked by running the prism soluble matrix on mini-gel, and by transferring it on PVDF membrane. The membrane was then incubated with the anti-caspartin serum, extensively rinsed, incubated with the second antibody (peroxidase conjugate Goat Anti-Rabbit, Sigma A6154), rinsed and revealed by luminol chemoluminescent staining [24].

2.3. Protein sequencing

A caspartin extract was *de novo* sequenced [25] at the Biology Department of the Technion (Smoler Proteomics Center), Haifa, with an electrospray-quadrupole-TOF mass spectrometer (Q-TOF Ultima, Micromass, UK). To this end, the caspartin extract was digested either by trypsin, either by pepsin or by aspN. This yielded peptides of different lengths, the sequences of which were determined. Sequences were analyzed for homology search in SwissProt database. A complementary analysis was performed with SIM computer program (http://www.expasy.ch/tools/sim-prot.html), by aligning two per two each obtained sequence with each of the 43 known full-length shell proteins, characterized by their SwissProt accession number.

2.4. Immunogold localization of caspartin

Following titer determination, the 2nd antiserum preparation was used for localizing caspartin in the prismatic layer. All the incubation steps were performed in Falcon multiwell tissue culture flat bottom plates (12 or 24 wells). NaOCl-isolated prisms or shell fragments were used for the

experiments. For the shell fragments, different surface pre-treatments were applied: untreated freshly broken pieces of prismatic layer; EDTA-etched freshly broken pieces of prismatic layer; mirror-polished sections, which were subsequently cleaned with dilute sodium hypochlorite (0.2 wt% active chlorine, 10 min) for removing antigens spread on the surface, rinsed with water, then slightly etched with EDTA. Etching with EDTA 1% (w/v), pH 7.5, during 2–3 min, allows the exposure of epitopes, and their subsequent recognition by the antibodies. Contrarily to a soft tissue preparation, the mineral surface does not need to be fixed. All preparations were blocked at least 30 min with filtered gelatine (0.5–1% w/v) dissolved in Tris buffered saline (TBS), with a pH readjusted at 7.5 with dilute sodium hydroxide solution, to avoid further dissolution of the calcium carbonate. This operation precludes non-specific bindings of antibodies. The preparations were subsequently incubated for a few hours to overnight with the antiserum raised against caspartin, diluted 1:3000 in a solution of 1% gelatine dissolved in TBS, pH 7.5, containing Tween 20 (0.05% v/v). For overnight incubations, NaN_3 (0.01% w/v), a bactericidal agent, was added to the solution. The preparations were extensively rinsed with TBS–Tween (4–6 times 10 min). They were subsequently incubated for 2–3 h in a small volume of the secondary antibody (Goat Anti-Rabbit coupled to 5-nm gold particles, British Biocell International, catalogue number EM.GAR5), diluted 400 times in 0.5% gelatin/TBS–Tween solution, pH 7.5. After extensive rinsing with TBS–Tween (4–6 times 10 min), the preparations were briefly rinsed with milli-Q water and dried before being silver enhanced at neutral pH [26] for 15–20 min with a silver enhancing kit (British Biocell International, catalogue number SEKL15). The staining was stopped, by rinsing the preparations with water. They were subsequently dried at 45 °C overnight and carbon sputtered (10 nm thick) for microscopic observations.

To check the specificity of the staining, blank experiments were performed similarly without the first antibody step or with pre-immune serum, diluted 1:3000. Samples were observed with a JEOL JSM 6400F (Dijon). Observations were made in the back-scattering electron mode, with a 7.5–10 KeV beam. The immunogold experiments were performed several times.

3. Results

3.1. The calcitic prisms of P. nobilis

As shown in Fig. 1, the prismatic outer layer of *P. nobilis* (Fig. 1A) is constructed from the dense packing of calcitic needles, which exhibit a polygonal section, the prisms (Fig. 1B). The prisms grow inwards from the periostracal layer, perpendicularly to the outer surface of the shell, and perpendicularly to nacre tablets (Fig. 1C). This direction corresponds to the crystallographic *c*-axis of the prisms. They are all maintained together by an organic framework, about 1 μm thick. This honeycomb-like structure is composed of framework proteins, which can be entirely destroyed by sodium hypochlorite. This treatment dissociates the prismatic layer in single prisms units (Fig. 1D and E). The length of each prism varies between few tens of microns and more than 1 mm, for a diameter comprised between 30 and 100 μm. They exhibit a layering perpendicular to their *c*-axis (Fig. 1E). The prisms of *P. nobilis* are defined as the "simple prisms" according to the terminology of Taylor et al. [27] and are known to behave

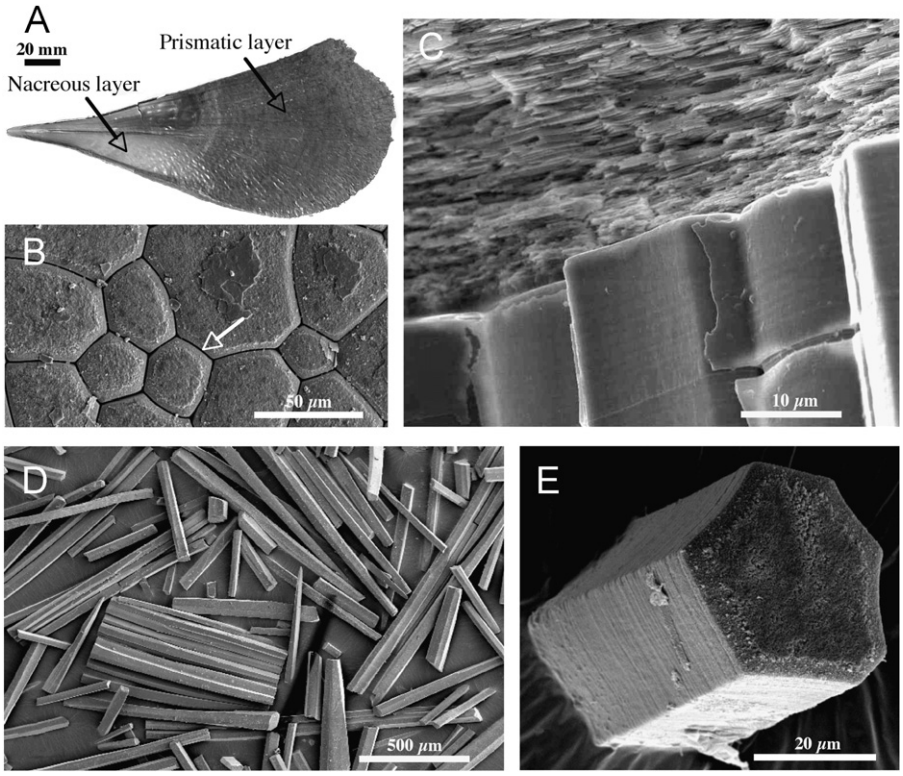

Fig. 1. Shell structure of *Pinna nobilis*: (A) macroscopic view of the internal surface of a right valve from a 2-year-old specimen, (B) non-cleaned surface of the prismatic layer, internal view. The densely packed prisms are maintained together by a thin interprismatic matrix (arrow), (C) transition zone between the prisms (down) and the nacre layer (top), transverse section, (D) isolated prisms from an adult specimen and (E) single prism, isolated with sodium hypochlorite. Note the thin layering perpendicular to the *c*-axis of the prism.

like monocrystals [27] although they exhibit several substructures [28]. For caspartin isolation and sequencing, antibody production, SDS-PAGE and Western blots, we used only the acetic acid-soluble matrix extracted from "within" the isolated prisms: this matrix should therefore be considered as *intracrystalline*.

3.2. Polyclonal antibodies against caspartin

On mini SDS-PAGE gel stained with silver nitrate, two prominent bands, localized by bold arrows, characterize the acetic acid-soluble matrix of the prisms of *P. nobilis* (Fig. 2, lane 2). In addition, several thin bands (small arrows) and a smear are also visible. The lower thick band, which migrates at 17 kDa of apparent molecular weight, corresponds to caspartin, an Asp-rich protein, the biochemical characteristics of which were described elsewhere [24]. Caspartin was purified from the crude soluble extract of NaOCl-isolated prisms, according to a previously published method [24]. It was tested for checking its purity on the same gel (Fig. 2, lane 3), and the purified extract was used for polyclonal antibody production. The anti-caspartin antibodies were tested by Western blot against the whole acetic acid-soluble prism matrix, at increasing matrix amounts. The results, shown in Fig. 2, lanes 4–6, indicate immuno-reactivity with a single band at 17 kDa, and no immunological cross-reactivity with the rest of the matrix. This strongly suggests that caspartin is the only matrix protein, recognized by the antibody preparation. The antibody preparation can thus be used for subsequent localization of caspartin directly in/on calcitic prisms.

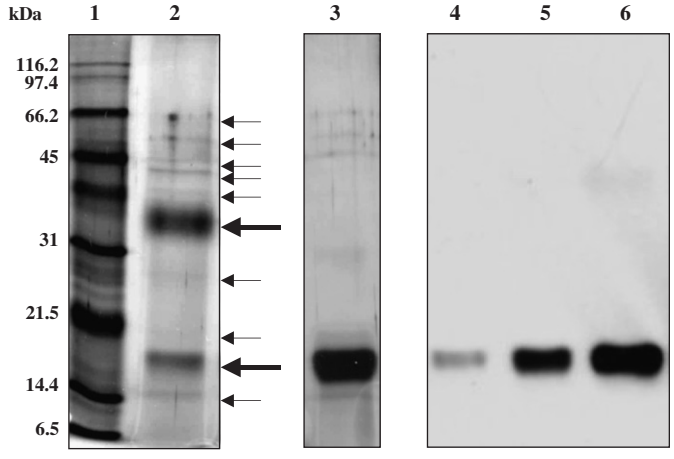

Fig. 2. SDS-PAGE (lanes 1–3) and Western blot (lanes 4–6) of the acetic acid-soluble matrix extracted from the prisms. Lane 1: broad range molecular weight standards. Lane 2: acetic acid-soluble matrix (SM) of the prisms of *Pinna nobilis*, 20 μg. Lane 3: purified caspartin, 10 μg. Lanes 1–3 were stained with silver nitrate. Lanes 4–6: SM of the prisms of *Pinna nobilis*, 5 μg (lane 4), 10 μg (lane 5), 20 μg (lane 6). The Western blots of lanes 4–6 were incubated with the anti-caspartin polyclonal antibody solution (dilution 1:3000). The signal obtained is very specific for caspartin.

3.3. Protein sequencing

The enzymatic digestions of caspartin generated peptides of different sizes (Fig. 3). A single acidic peptide was obtained after the trypsin digestion. This 17-residues peptide exhibits six aspartic acid residues (Fig. 3A). The pepsin digestion yielded five peptides (9–12 residues). Two of them differ only by one residue (M/F) in their C-terminus, and the three others, by three residues (Fig. 3B). Finally, the aspN digestion produced three additional almost identical peptides of 13 residues each, which differ by two residues in their N-terminus (Fig. 3C). These almost identical peptides produced by one enzymatic digestion may represent isoforms of a single domain or repeat units. A homology search performed with BLAST did not give significant results. However, the complementary SIM analysis, made by aligning two per two each obtained sequence with each of all the known full-length molluscan shell proteins (43 different accession numbers in SwissProt, including all the variants of Asp-rich and of shematrin families), produced interesting matching motifs. Among them, 17 have three consecutive amino acids, three have four amino acids (DAAD, SLSA, AVTA), and one, five residues (DAADV). The sequence of the acidic peptide obtained after the trypsin digestion exhibits some similarities with the sequences of the most acidic shell proteins, namely aspein, Asp-rich and MSP-1 (Fig. 3D). All three proteins are found in association with calcitic shell textures [29]. The peptide obtained from the pepsin digestion

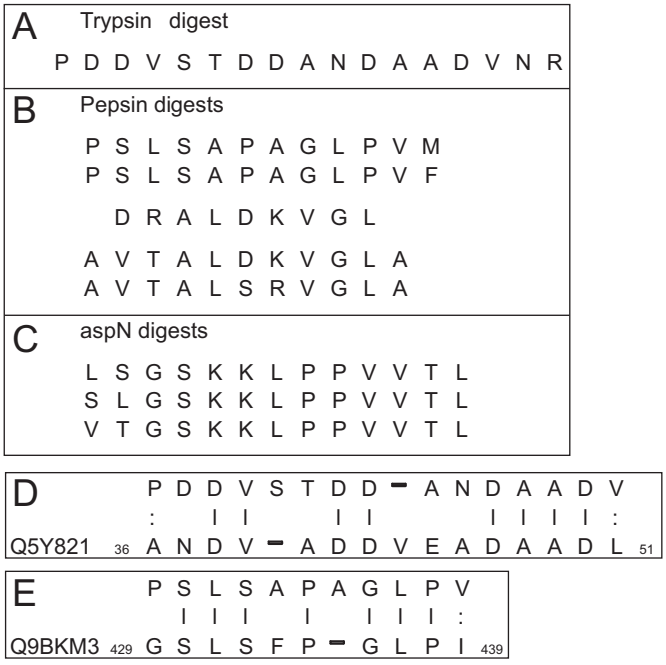

Fig. 3. Partial amino acid sequences obtained by *de novo* sequencing, after digestion: with trypsin (A), with pepsin (B), with aspN (C). (D) Sequence alignment of the trypsin digest with one of the members of the Asp-rich family (SwissProt accession number Q5Y821). (E) Sequence alignment of the pepsin digest with mucoperlin (SwissProt accession number Q9BKM3).

(PSLSAPAGLPV) exhibits some similarities with the C-terminus of mucoperlin (Fig. 3E), a mucin-like protein, which is specific of the nacreous layer of *P. nobilis* [22]. Taken together, our sequence data show that the primary structure of caspartin is constituted of domains, which markedly differ in their hydrophobicity/hydrophilicity. This suggests that these domains may display different functions in biomineralization.

3.4. Immunogold staining

The results of the immunogold staining are shown in Figs. 4 and 5. In the back-scattered electron mode, the gold particles, which are covalently bound to the secondary antibody (goat anti-rabbit), appear as tiny bright spots. The diameter of the spots depends on the duration of the silver enhancement. Typically, the spot size is comprised between 50 and 100 nm after 20 min incubation in the silver enhancement solution.

In our hands, we found that the use of secondary antibodies coupled with small gold particles—5 or 1 nm diameter—gave the best results. Attempts to use 30 nm gold particles were not successful, since very weak signals were obtained (not shown). This suggests that the size of the gold particles may induce steric or charge hindrance, as described by the manufacturer. Furthermore, we found that the best observations were performed at 7.5 or 10 KeV: attempts at 5 KeV gave low signal; at 15 KeV, thick samples had a tendency to charge.

Another parameter to check is the pH of the different gelatin solutions. In standard immunological tests (ELISA, Dot blot, Western blot), pH values of the gelatin solutions are usually not readjusted. A 1% gelatin solution significantly lowers the pH (below pH 6). Because we

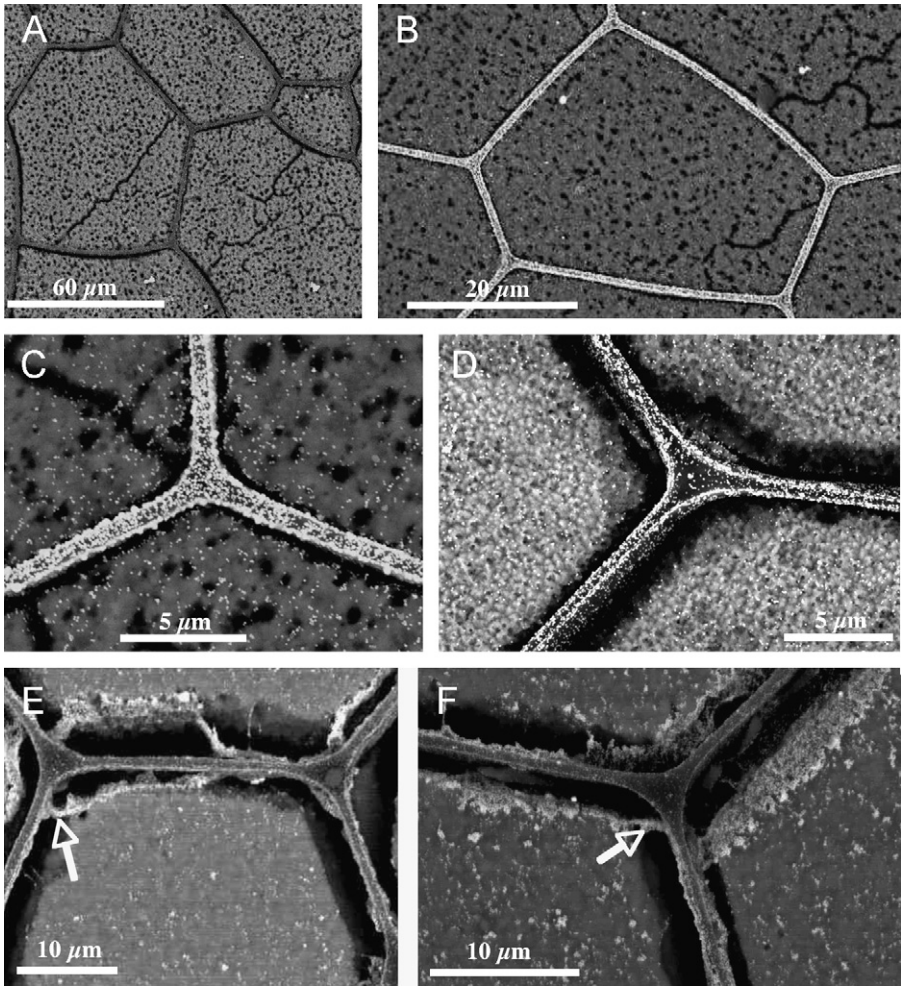

Fig. 4. Immunogold staining of transverse sections of prisms preparations, observed by scanning electron microscope, in back-scattered electron mode. Different preparations were tested: (A) negative control obtained on a fresh fracture, short etching (1 min) with EDTA, and incubation with pre-immune serum. (B) Similar preparation incubated with the anti-caspartin antiserum. Note the differences between A and B: in B, the surface of the prisms is stained, as well as a double layer, which surrounds each prism. (C) Triple junction between three prisms; same treatment as B. The double coating is evident, as well as a staining on the surfaces of the prisms. (D) Similar triple junction of a sample etched for 5 min. The dissolution takes place at the interface between the prisms and the insoluble sheaths. (E and F) Similar preparation, obtained after a long etching time (20 min). A densely stained membrane (arrow) is observed at the interface between the prisms and the organic periprismatic sheaths. In F, one of the densely stained lateral sides of a prism is clearly visible (arrow).

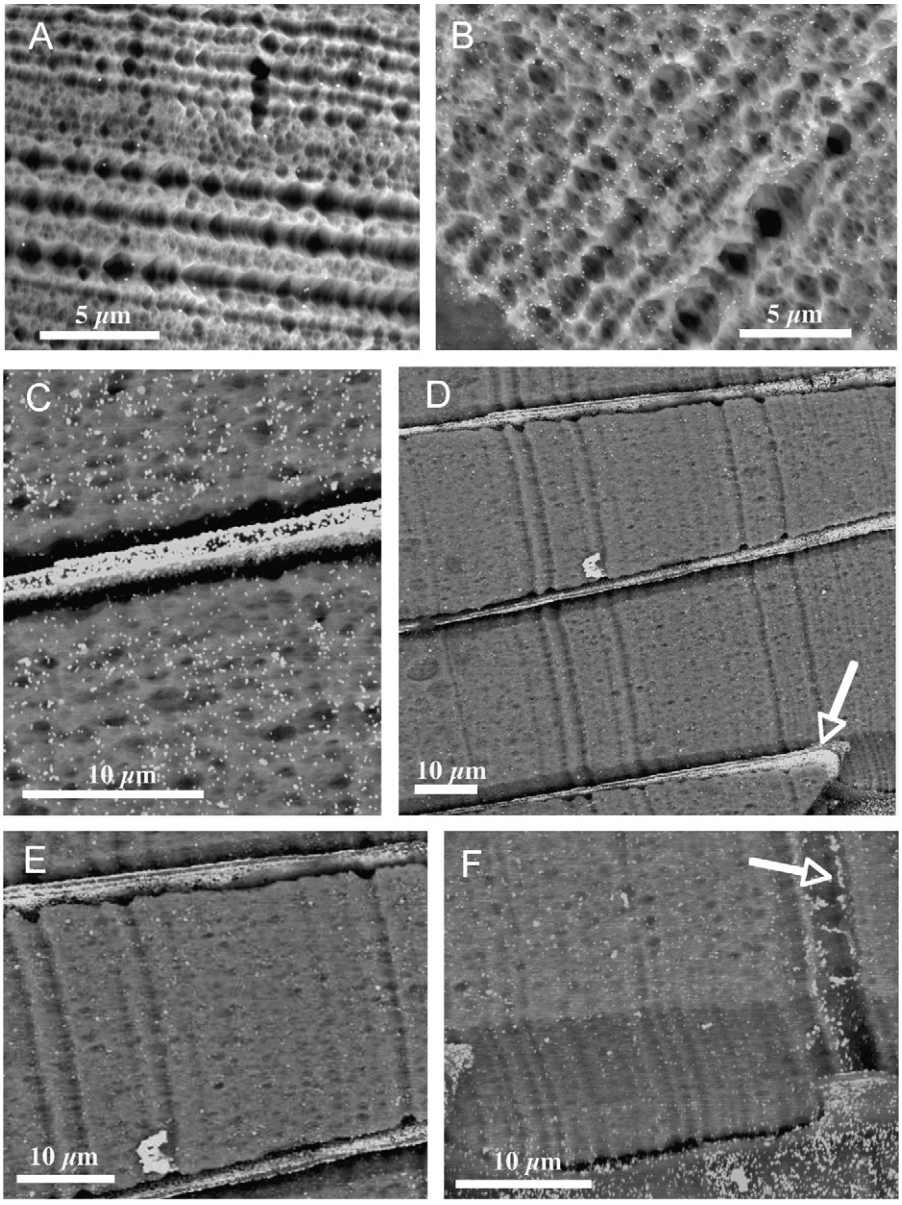

Fig. 5. Immunogold staining on isolated prisms (A and B) and on longitudinal section of prisms (C–F). (A) Negative control, single prism incubated with the pre-immune serum. Few background spots are visible. (B) Single prism preparation, obtained after extensive NaOCl treatment, then rinsed, briefly etched with EDTA and incubated with the anti-caspartin antiserum. The staining is less dense than in Fig. 5C, due to caspartin removal by NaOCl treatment. (C) Longitudinal section, EDTA-etching, 5 min. Caspartin makes a double layer around the prisms and is also densely spread on the surface. (D–F) Longitudinal section, EDTA-etching, 10 min: (D) the caspartin-rich layer around the prism can be clearly seen (arrow), (E) same as D, higher magnification and (F) although most of the immunogold signal is spread along the prism, a caspartin-rich discontinuous 'layer' is observed on the right side (arrow).

work with $CaCO_3$ biominerals and gelatin is used in three incubation steps (for blocking and for the two antibody solutions), we advise to maintain pH at 7–7.5 with sodium hydroxide, for precluding the formation of dissolution patterns (particularly visible on single prism preparations, not shown), and a significant decrease of the immunological signal. In all our experiments, we buffered the gelatin solutions at pH 7.5.

We prepared different surface treatments to check whether the obtained images were not artifacts. For example, we observed that polishing the samples, rinsing and etching with EDTA, blocking with gelatin and incubating with the first antibody solution induced artifacts, since the polishing provoked a spreading of the antigens on the surface of the polished surface. This can be solved by adding an extra-step of surface cleaning with dilute sodium hypochlorite (bleaching), after the polishing and before rinsing with water and etching with EDTA (Fig. 4D–F). We compared the results obtained with those obtained on freshly broken pieces, which were directly etched with EDTA, blocked with gelatin and treated with the first antibody solution (Fig. 4B and C). They were not

significantly different. Thus, we recommend working with freshly broken and EDTA-etched surfaces, this treatment minimizing the possibilities of artifacts.

Fig. 4 corresponds to transverse sections of prisms (plane perpendicular to the *c*-axis of the prisms). It shows that caspartin is distributed as a continuous double layer coating the two sides of the insoluble organic sheaths that surround the crystals (Fig. 4B–F). The different treatments applied to the shell surface do not fundamentally affect the distribution pattern of caspartin. Fig. 4B and C are produced on freshly broken pieces, with an extremely brief etching (1 min). Fig. 4D corresponds to another preparation, which was EDTA-etched for 5 min and Fig. 4E and F correspond to an EDTA-etching treatment of 20 min, which results in the formation of an empty space due to prism dissolution, between the prisms and the insoluble sheath. Interestingly, this last preparation clearly shows that caspartin makes a continuous film at the interface between the prisms and the sheaths (white arrows). It also shows that the film is maintained coherent in spite of being detached from its sheath template (Fig. 4F). This suggests that the caspartin, which constitutes the interfacial film, may be in an insoluble form, by polymerization or by strong interaction with other insoluble film components. In transverse sections, caspartin is also densely distributed on the top surface of the prisms (Fig. 4C, D and F). On this surface, the distribution of caspartin looks homogeneous, and this protein does not seem to be preferentially concentrated in specific zones. The different durations of the EDTA-etching do not affect the distribution of caspartin and the density of spots, on top of the prisms surface. The most likely explanation is that, because intracrystalline caspartin is more or less homogeneously distributed within the prisms, the EDTA etching treatment continuously unmasks 'new' embedded caspartin molecules during the slow dissolution of the prisms surface.

Fig. 5 shows the distribution on caspartin, either on the surface of isolated prisms (Fig. 5B) or on longitudinal polished sections (sections parallel to the *c*-axis of the prisms, Fig. 5C–F). Fig. 5C and E confirm the staining of a double layer coating the insoluble sheath, at the interface with the mineral phase. The caspartin film can be observed on the partly unmasked peri-prismatic sheath of Fig. 5D (bottom, white arrow). Numerous bright spots are also scattered within the prisms (Fig. 5B, C and F). On longitudinal view of isolated prism preparations (Fig. 5B), caspartin is slightly less densely distributed than in polished sections (Fig. 5C), which suggests that the NaOCl treatment used for isolating the prisms may partly degrade caspartin. The distribution of caspartin on polished sections is more or less uniform and does not follow the planes corresponding to the growth increments of the prisms. Only in few cases, caspartin is more concentrated in certain planes, perpendicular to the axis of the prisms (Fig. 5F, white arrow). However, the caspartin distribution along these planes is not continuous, which suggests that caspartin does not make a 'template' film, as it is the case for the 'peri-prismatic' caspartin. In all our experiments, the negative controls always produce a low background (Fig. 4A and 5A).

4. Discussion

The present paper describes partial sequences of caspartin and the localization of this protein on and within calcium carbonate biominerals by immunogold staining followed by observation with SEM. Our previous incomplete biochemical characterization suggested that caspartin is an aspartic acid-rich protein [24]. Our conclusions were based on the amino acid composition of caspartin, obtained after acid hydrolysis. In the absence of sequence data, we did not exclude the possibility that a part of the aspartic acid residues detected come from the conversion of asparagine residues during the hydrolysis, and that caspartin might be less acidic than initially suspected. In this paper, the partial sequence obtained after trypsin digestion reveals one Asp-rich domain, which shows similarities with one found in the Asp-rich family [29]. On the other hand, the other peptides (generated by aspN or pepsin digestions) are more hydrophobic: the aspN peptides exhibit two consecutive lysine residues and a short hydrophobic motif. This domain might be involved in the anchoring of caspartin to the framework insoluble sheath, as suggested for the basic C-terminal domain of lustrin A [30]. Furthermore, the presence of hydrophobic domains in an acidic protein, which inhibits the growth of calcium carbonate in solution, is known to enhance its inhibitory capacity [31]. Finally, two of the peptides produced by the pepsin digestion exhibit some similarities with mucoperlin [22], a protein specific of the nacre layer of *P. nobilis*. Although this similarity is not well understood at the functional level, it suggests that short protein domains can be re-used as 'building blocks' by different mineralizing proteins with different functions.

Caspartin was also localized by immunogold. The technique combines the specificity of the antigen–antibody reaction to observation at high magnification. The immunogold–SEM technique has been used for localizing specific antigens on cell membranes [32,33] or bioactive components on the surface of tailored materials [34,35]. However, the combination of immunogold labeling and SEM observation has been applied to $CaCO_3$ biominerals in rare cases: mollusk shell [24,36] and sea urchin spicules [37–39]. This technique brings invaluable information on the 3D relationships between matrix components and the mineral itself, at the 'mesoscale' [39]. It can be applied to all kinds of biominerals of prokaryotic or eucaryotic origin, fresh or fossil, provided that a specific antibody is available. Furthermore, by combining different antibodies raised against different matrix macromolecules, a biomineral protein mapping becomes technically feasible.

The localization of caspartin in the prisms by immunogold calls for further explanation. Since the pioneering work of Crenshaw [40], it is common knowledge to

distinguish shell proteins according to their solubility in the decalcifying solution. One distinguishes the 'soluble' proteins, which are hydrophilic and rich in aspartate residues, and the 'insoluble' proteins, which are hydrophobic, because of their high content in aliphatic amino acid. To this "technical" classification is superimposed another one introduced by Crenshaw: the *intercrystalline* versus *intracrystalline* fractions. The *intercrystalline* matrix corresponded to the EDTA-insoluble components localized around the calcium carbonate crystallites, and easily destroyed by a NaOCl treatment. The *intracrystalline* fraction corresponded to the EDTA-soluble proteins, protected from NaOCl because of their location within the biocrystals. According to this and to the protocol used for prisms isolation, caspartin is *intracrystalline*. However, the simple view that associates hydrophilicity to *intracrystallinity* and hydrophobicity to *intercrystallinity* is inadequate. Our immunogold localization experiment shows that caspartin is both *intracrystalline* (dispersed within the crystals) and *intercrystalline* (forming a film at the periphery of the prisms). In a previous study on sea urchin, it was similarly shown that two soluble spicule proteins, SM50 and SM30, were both intracrystalline and located on the surface of the biocrystals [39]. Furthermore, our study demonstrates that the interprismatic framework is a three-layered structure, with the framework taken as sandwich between two caspartin-rich films. Such an organization had been described for nacre [17] but never for prisms. The single indication so far that the interprismatic framework may be heterogeneous comes from one recent paper [28], but the evidence presented is scanty and indirect. Our data unambiguously clarify this point.

We can try to relate the location of caspartin to its putative roles in the prisms biomineralization process.

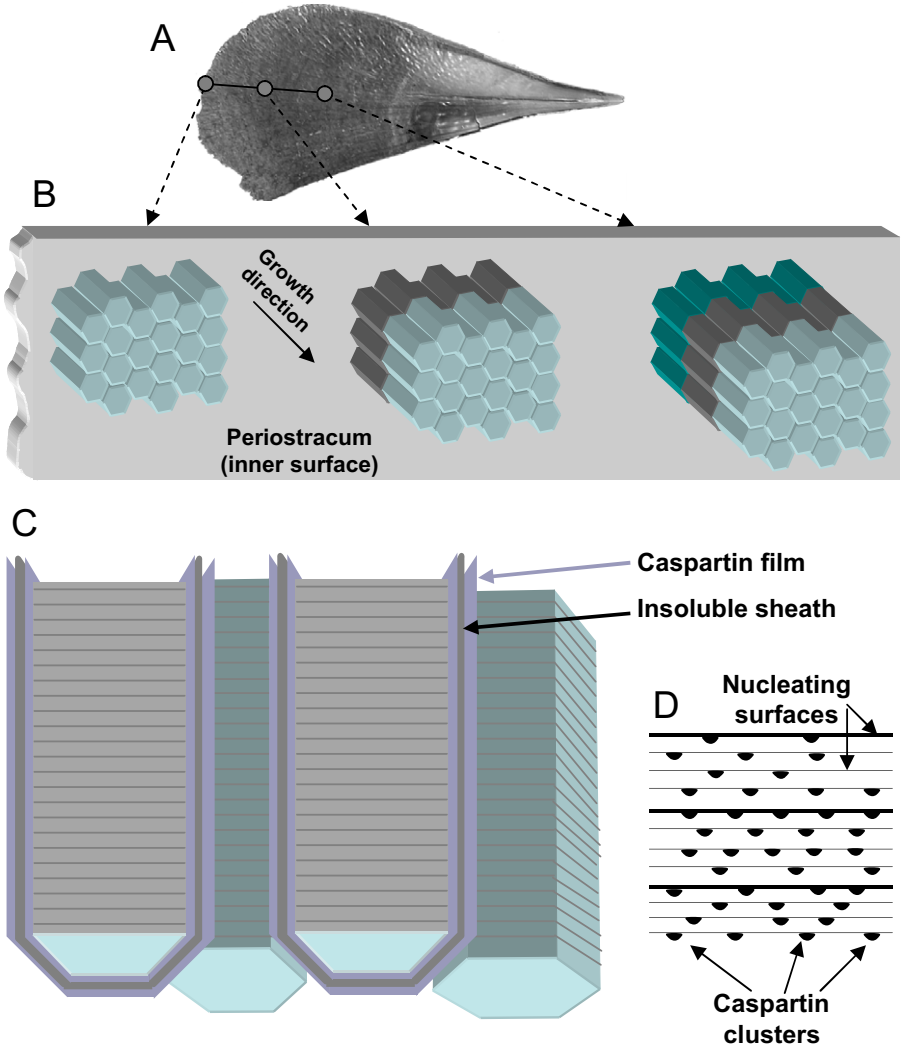

Fig. 6. A simplified model of the putative functions of caspartin, according to its location within and around the calcitic prisms of *Pinna nobilis*. (A) The inner surface of the shell is observed. (B) Schematic view of three groups of prisms, at different growth stages. The periostracum, secreted by the cells of the periostracal groove, is the organic membrane from which prisms grow. (C) Detailed scheme of five prisms. Each prism is initiated as a spherulite, which first grows centripetally (not represented). Caspartin makes a double coating film around each prism. (D) Detail of C. The "intracrystalline" caspartin may act as a nucleator of nanocrystals on the growing surface of each prism.

Because caspartin has basically two locations *around* and *within* calcitic prisms, different functions should be considered as shown by Fig. 6. At first, the *intracrystalline* caspartin may act as a nanocrystal nucleator, on the growing surfaces of each prism. If so, the nucleating surface would not be a continuous template of caspartin, but rather a mineral surface punctuated by caspartin clusters (Fig. 6D), from which nucleated nanocrystals would coalesce. As a consequence of its *intracrystalline* localization, caspartin is a crystal lattice modifier. We recently observed that caspartin, when incorporated to calcite grown *in vitro*, induces a slight lattice distorsion, especially along the *c*-axis, when compared to non-biogenic calcite [41]. Secondly, the *intercrystalline* caspartin film may also display different functions. Firstly, it would act as an inhibiting surface, which may help to constrain the growth of the crystal in the *c*-axis direction (Fig. 6B and C). Secondly, caspartin may be involved in maintaining the crystallographic orientation of the whole prism. However, the mechanism by which this would be performed is unclear. Thirdly, the caspartin film coated on the interprismatic walls acts as a "polyanionic sink", for sequestering calcium ions or for driving bicarbonate ions to the nucleating surface. A very elegant alternative hypothesis, published recently [42], proposes that the interprismatic hydrophobic walls are shaped by interfacial tension that occurs in a precursor liquid–liquid emulsion. If so, the hydrophilic caspartin may play an active role in this self-assembling process: being localized as a film at the surface of the liquid droplets of the extrapallial fluid, it may stabilize the emulsion, while the more viscous and hydrophobic organic phase polymerizes in a solid but flexible honeycomb-like structure.

5. Conclusion

Clearly, if obtaining the location of a protein in/on a biomineral is not *per se* a sufficient condition for understanding the biomineralization process, it constitutes an invaluable information for assessing putative functions of this protein.

Acknowledgments

This work was initiated in the Dutch Biotech Company IsoTis (Bilthoven) and continued in Dijon. This paper is a contribution to an "Aide Concertée Incitative Jeunes Chercheurs" (ACI JC 3049) awarded to F. Marin by the French "Ministère Délégué à la Recherche et aux Nouvelles Technologies". In 2004, the "Conseil Régional de Bourgogne" (Dijon, France) provided additional supports for the acquisition of new equipment in Biogeosciences research unit. F.M. thanks Claudie Josse (Laboratoire de Réactivité des Solides, UB, Dijon) for her help in handling SEM. F. Marin and B. Pokroy thank the Smoler Proteomics Center at the Department of Biology of Technion, Haifa, for their help in performing the *de novo* sequencing, and Prof. Noam Adir (Chemistry, Technion) and Prof. Emil Zolotoyabko (Materials Engineering, Technion) for helpful discussions.

References

[1] Mann S. Biomineralization. Principles and concepts in bioinorganic materials chemistry. Oxford: Oxford University Press; 2001.
[2] Mayer G. Rigid biological systems as models for synthetic composites. Science 2005;310:1144–7.
[3] Begley CT, Doherty MJ, Mollan RA, Wilson DJ. Comparative study of the osteoinductive properties of bioceramic, coral and processed bone graft substitutes. Biomaterials 1995;16:1181–5.
[4] Atlan G, Balmain N, Berland S, Vidal B, Lopez E. Reconstruction of human maxillary defects with nacre powder: histological evidence for bone regeneration. CR Acad Sci Paris 1997;320:253–8.
[5] Lowenstam HA, Weiner S. On biomineralization. New York: Oxford University Press; 1989.
[6] Weiner S, Addadi L. Design strategies in mineralized biological materials. J Mater Chem 1997;7:689–702.
[7] Miyamoto H, Miyashita T, Okushima M, Nakano S, Morita T, Matsushiro A. A carbonic anhydrase from the nacreous layer in oyster pearls. Proc Natl Acad Sci USA 1996;93:9657–60.
[8] Westbroek P, Marin F. A marriage of bone and nacre. Nature 1998; 392:861–2.
[9] Weiner S, Traub W. Macromolecules in mollusk shells and their functions in biomineralization. Philos Trans R Soc Lond B 1984;304:424–5.
[10] Schäffer TE, Ionescu-Zanetti C, Proksch R, Fritz M, Walters DA, Almqvist N, et al. Does abalone nacre form by heteroepitaxoial nucleation or by growth through mineral bridges? Chem Mater 1997; 9:1731–40.
[11] Levi-Kalisman Y, Falini G, Addadi L, Weiner S. Structure of the nacreous organic matrix of a bivalve mollusk shell examined in the hydrated state using cryo-TEM. J Struct Biol 2001;135:8–17.
[12] Nassif N, Pinna N, Gehrke N, Antonietti M, Jäger C, Cölfen H. Amorphous layer around aragonite platelets in nacre. Proc Natl Acad Sci USA 2005;102:12653–5.
[13] Addadi L, Joester D, Nudelman F, Weiner S. Mollusk shell formation: a source of new concepts for understanding biomineralization processes. Chem Eur J 2006;12:980–7.
[14] Götze J. Potential of cathodoluminescence (CL) microscopy and spectroscopy for the analysis of minerals and materials. Anal Bioanal Chem 2002;374:703–8.
[15] Gautret P, Reitner J, Marin F. Mineralization events during growth of the coralline sponges *Acanthochaetetes* and *Vaceletia*. Bull Inst Oceanogr Monaco No special 14 1996;4:325–34.
[16] Mutvei H. The nacreous layer in molluscan shells. In: Omori M, Watabe N, editors. The mechanisms of biomineralization in animals and plants. Tokyo: Tokai University Press; 1980. p. 49–56.
[17] Nakahara H. Nacre formation in bivalve and gastropod mollusks. In: Suga S, Nakahara H, editors. Mechanisms and phylogeny of mineralization in biological systems. Tokyo: Springer; 1991. p. 343–50.
[18] Walters DA, Smith BL, Belcher AM, Paloczi GT, Stucky GD, Morse DE, et al. Modification of calcite crystal growth by abalone shell proteins: an atomic force microscope study. Biophys J 1997;72: 1425–33.
[19] Dauphin Y, Cuif JP, Doucet J, Salomé M, Susini J, Williams CT. In situ chemical speciation of sulfur in calcitic biominerals and the simple prism concept. J Struct Biol 2003;142:272–80.
[20] Fayek M, Utsunomiya S, Pfiffner SM, White DC, Riciputi LR, Ewing RC, et al. The application of HRTEM and NanoSIMS to chemically and isotopically characterize *Geobacter sulfurreducens* surfaces. Can Mineral 2005;43:1631–41.
[21] Muyzer G, Westbroek P. An immunohistochemical technique for the localization of preserved biopolymeric remains in fossils. Geochim Cosmochim Acta 1989;53:1699–702.

[22] Marin F, Corstjens P, De Gaulejac B, De Vrind-De Jong E, Westbroek P. Mucins and molluscan calcification: molecular characterization of mucoperlin, a novel acidic mucin-like protein of the nacreous shell-layer of the fan mussel *Pinna nobilis* (Bivalvia, Pteriomorphia). J Biol Chem 2000;275:20667–75.
[23] Puverel S, Tambutté E, Zoccola D, Domart-Coulon I, Bouchot A, Lotto S, et al. Antibodies against the organic matrix in scleractinians: a new tool to study coral biomineralization. Coral Reefs 2005;24: 149–56.
[24] Marin F, Amons R, Guichard N, Stigter M, Hecker A, Luquet G, et al. Caspartin and calprismin, two proteins of the shell calcitic prisms of the Mediterranean fan mussel *Pinna nobilis*. J Biol Chem 2005;280: 33895–908.
[25] Standing KG. Peptide and protein *de novo* sequencing by mass spectrometry. Curr Opin Struct Biol 2003;13:595–601.
[26] Robinson JM, Takizawa T, Vandré DD, Burry RW. Ultrasmall immunogold particles: important probes for immunocytochemistry. Microsc Res Tech 1998;42:13–23.
[27] Taylor JD, Kennedy WJ, Hall A. The shell structure and mineralogy of the Bivalvia. Introduction. Nuculacea—Trigonacea. Bull Brit Mus (Nat Hist) 1969; (Suppl. 3): 1–125.
[28] Dauphin Y. Comparison of the soluble matrices of the calcitic prismatic layer of *Pinna nobilis* (Mollusca, Bivalvia, Pteriomorpha). Comp Biochem Physiol 2003;A132:577–90.
[29] Gotliv BA, Kessler N, Sumerel JL, Morse DE, Tuross N, Addadi L, et al. Asp-rich: a novel aspartic acid-rich protein family from the prismatic shell matrix of the bivalve *Atrina rigida*. ChemBioChem 2005;6:304–14.
[30] Shen X, Belcher AM, Hansma PK, Stucky GD, Morse DE. Molecular cloning and characterization of lustrin A, a matrix protein from the shell and pearl nacre of *Haliotis rufescens*. J Biol Chem 1997;272:32472–81.
[31] Sikes CS, Yeung ML, Wheeler AP. Inhibition of calcium carbonate and phosphate crystallization by peptides enriched in aspartic acid and phosphoserine. In: Sikes CS, Wheeler AP, editors. Surface reactive peptides and polymers. Washington: American Chemical Society; 1991. p. 50–71.
[32] Hermann R, Walther P, Müller M. Immunogold labeling in scanning electron microscopy. Histochem Cell Biol 1996;106:31–9.
[33] Odendal M, Brady K, McDonald F. The localization of estrogen receptors on human osteoblasts: a preliminary optical and electron microscopic technique. Cell Biochem Biophys 2004;40:237–48.
[34] Park K, Simmons SR, Albrecht RM. Surface characterization of biomaterials by immunogold staining—quantitative analysis. Scann Microsc 1987;1:339–50.
[35] Sammons R, Marquis P. Application of the low vacuum scanning electron microscope to the study of biomaterials and mammalian cells. Biomaterials 1997;18:81–6.
[36] Nudelman F, Gotliv BA, Addadi L, Weiner S. Mollusk shell formation: mapping the distribution of organic matrix components underlying a single aragonitic tablet in nacre. J Struct Biol 2006;153: 176–87.
[37] Cho JW, Partin JS, Lennarz WJ. A technique for detecting matrix proteins in the crystalline spicule of the sea urchin embryo. Proc Natl Acad Sci USA 1996;93:1282–6.
[38] Ameye L, De Becker G, Killian C, Wilt F, Kemps R, Kuypers S, et al. Proteins and saccharides of the sea urchin organic matrix of mineralization: characterization and localization in the spine skeleton. J Struct Biol 2001;134:56–66.
[39] Seto J, Zhang Y, Hamilton P, Wilt F. The localization of occluded matrix proteins in calcareous spicules of sea urchin larvae. J Struct Biol 2004;148:123–30.
[40] Crenshaw MA. The soluble matrix from *Mercenaria mercenaria* shell. Biomineralization 1972;6:6–11.
[41] Pokroy B, Fitch AN, Marin F, Kapon M, Adir N, Zolotoyabko E. Anisotropic lattice distorsions in biogenic calcite induced by intra-crystalline organic molecules. J Struct Biol 2006;155:96–103.
[42] Checa AG, Rodriguez-Navarro AB, Esteban-Delgado FJ. The nature and formation of calcitic columnar prismatic shell layers in pteriomorphian bivalves. Biomaterials 2005;26:6404–14.